

Electronic Supplemental Information

Polypropylene-MWCNT Composite degradation, release, detection and toxicity of MWCNT during accelerated aging

Changseok Han^{1,2}, *E. Sahle-Demessie*^{2,*}, *Eunice Varughese*², *Honglan Shi*³

¹Department of Environmental Engineering, INHA University, Incheon 22212, Korea

²Oak Ridge Institute for Science and Education, Oak Ridge TN, 37831, United State

³U.S. Environmental Protection Agency, Office of Research and Development, National Risk Management Laboratory, Cincinnati, OH 45268, United State

³Missouri University of Science and Technology, Department of Chemistry, Rolla, MO, United State

* To whom correspondence should be addressed:

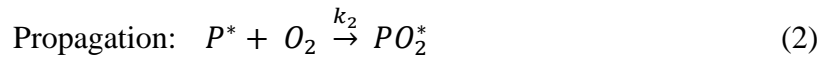
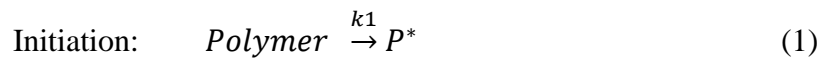
E. Sahle-Demessie: Tel:+1-513-569-7739; Fax: +1-513-569-7879;
E-mail: sahle-demessie.endalkachew@epa.gov

Contents

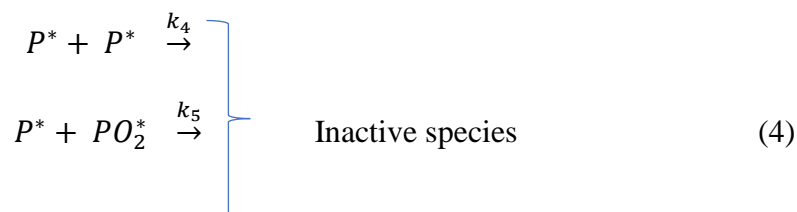
1	Theoretical Determination of Photooxidation of Polymer plates	2
S2.	Experimental	4
S3.	Analysis of MWCNT Released from Polymer Matrix using SP-ICP-MS.....	8

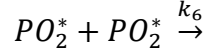
1 Theoretical Determination of Photooxidation of Polymer plates

Photooxidation of polymer nanocomposites is a multifaceted process of chemical reaction and surface erosion. Natural weathering is of a complex process. There is little information on the mathematical modeling of directly dedicated to the aging of PP-MWCNT, it is reasonable to modify existing models to incorporate aging effects. Degradation reaction is based on the initiation, propagation, and termination of radicals, resulting in the formation of more stable structures. The reactions depend on the irradiation of UV-vis light, the presence of oxygen and the extraction of hydrogen. Photooxidation in the aging chamber is the acceleration of natural reaction that involves absorption of UV light and the presence of atmospheric oxygen generates free radicals. Thus, aging reactions such as hydrolysis, photolysis, and oxidation are superficial and includes the reaction of O₂, H₂O, or oxidative radicals with the polymer causing disintegration. The solubility of oxygen in polypropylene at room temperature is sufficient for reactions to produce alkyl, alkoxy and peroxy radicals in the presence of UV light. The standard radical chain oxidation mechanism could be considered:



Termination:





Where P^* is the polymer radical, k_i are the reaction rates. Photooxidation of polymers forms photo reactive species such as $POOH$ where carbonyls play a significant role. The reaction of O_2 with P^* is fast. Thus, we can imagine fast kinetic regime where O_2 is sufficiently high, near the aging surface, and a lower kinetic regime where O_2 is lower than critical. The ketones that are formed by photo-oxidation can undergo Norrish I and Norrish II degradation [34]. Audouine et al., have shown that for high oxygen concentration [35],

$$-\frac{d[O_2]}{dt} \cong k_2 \left(r_i / k_6 \right)^{\frac{1}{2}} [PH] \quad (5)$$

For low oxygen concentrations

$$-\frac{d[O_2]}{dt} \cong k_2 \left(r_i / k_4 \right)^{\frac{1}{2}} [O_2] \quad (6)$$

For the UV aging the reaction rate $r_i = aI^{2\gamma}$ where a and γ are constants depending on the mechanism, and γ is usually between 0.5 and 1.0 for the chain mechanism. This reaction has diffusion-controlled kinetics, where the reaction rate is a function of the local concentration of the reactants. Hence, combining Fick's second law for small reactive molecules are consumed at a rate r with polymer molecules:

$$\frac{\partial C}{\partial t} = D \frac{\partial^2}{\partial x^2} - r \quad (7)$$

Where D is the coefficient of O_2 diffusion in the polymer. The reaction is a function of the local reactants concentration reaching a stationary state $r_i \rightarrow r(C)$ and when $\partial C / \partial t = 0$.

The reaction can be approximated as [36]:

$$r \sim r_o = k_2 C \sqrt{\frac{r_i}{k_4}} = KC \text{ with } K = k_2 \sqrt{\frac{r_i}{k_4}} \quad (8)$$

The initiation reaction depends on the light intensity Φ_i and light absorption.

$$r_i = \Phi_i I \quad (9)$$

Combining equations (9) and (7) and simplifying

$$D \frac{\partial^2 C}{\partial x^2} = K_o C \exp\left(\frac{x}{2X_i}\right) \quad (10)$$

The thickness of the oxidized layer (TOL) is a function of the light intensity Φ_i and oxygen diffusion:

$$TOL \cong \Phi^{-1} = \left(\frac{D}{k}\right)^{1/2} \quad (11)$$

Thus, oxygen penetration is the controlling factor for the penetration of degradation within the sample thickness.

S2. Experimental

Melting and mixing of PP and MWCNTs

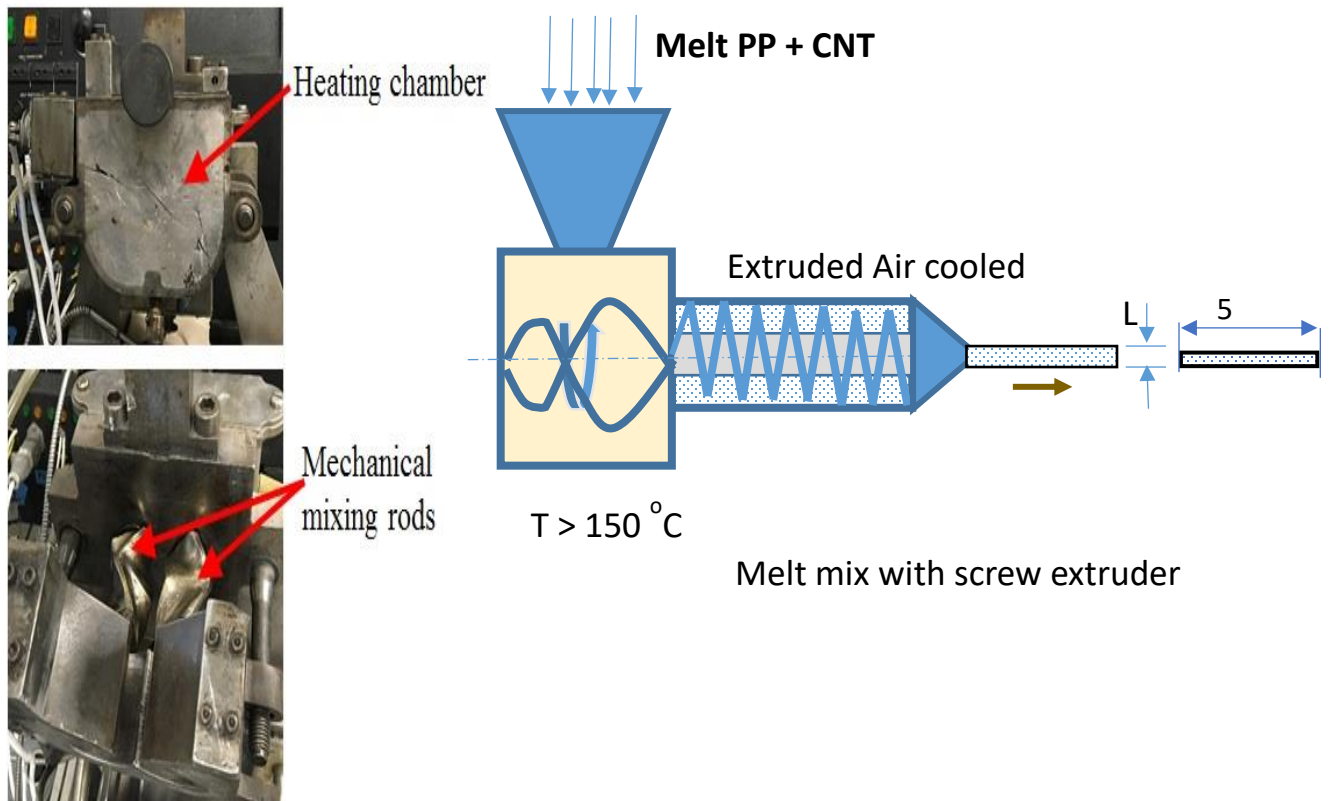


Figure S1 Experimental system used for preparing Polypropylene (PP) and PP-MWCNT rolls of selected thicknesses that were cut to make test plates

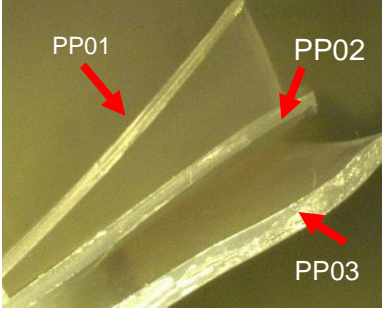
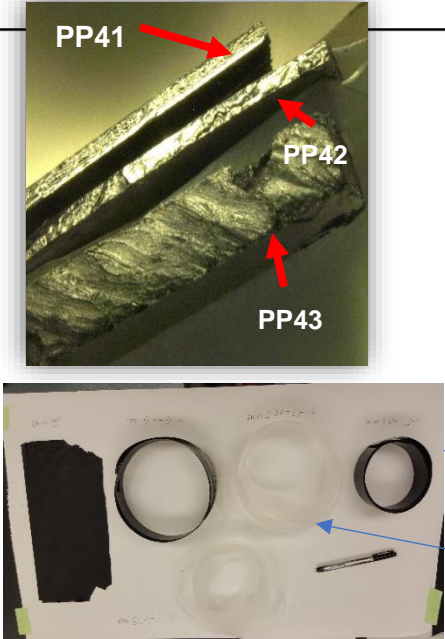
Material	Cross sectional Image	Sizes
Polypropylene		<p>PP01 = 0.25 ± 0.01 mm</p> <p>PP02 = 0.39 ± 0.02 mm</p> <p>PP03 = 0.69 ± 0.04 mm</p>
Polypropylene-MWCNT composite (4 wt%)		<p>PP41 = 0.35 ± 0.03 mm</p> <p>PP42 = 0.50 ± 0.01 mm</p> <p>PP43 = 2.07 ± 0.06 mm</p>

Figure S2 Cross-sectional images test materials PP, PP-MWCNT

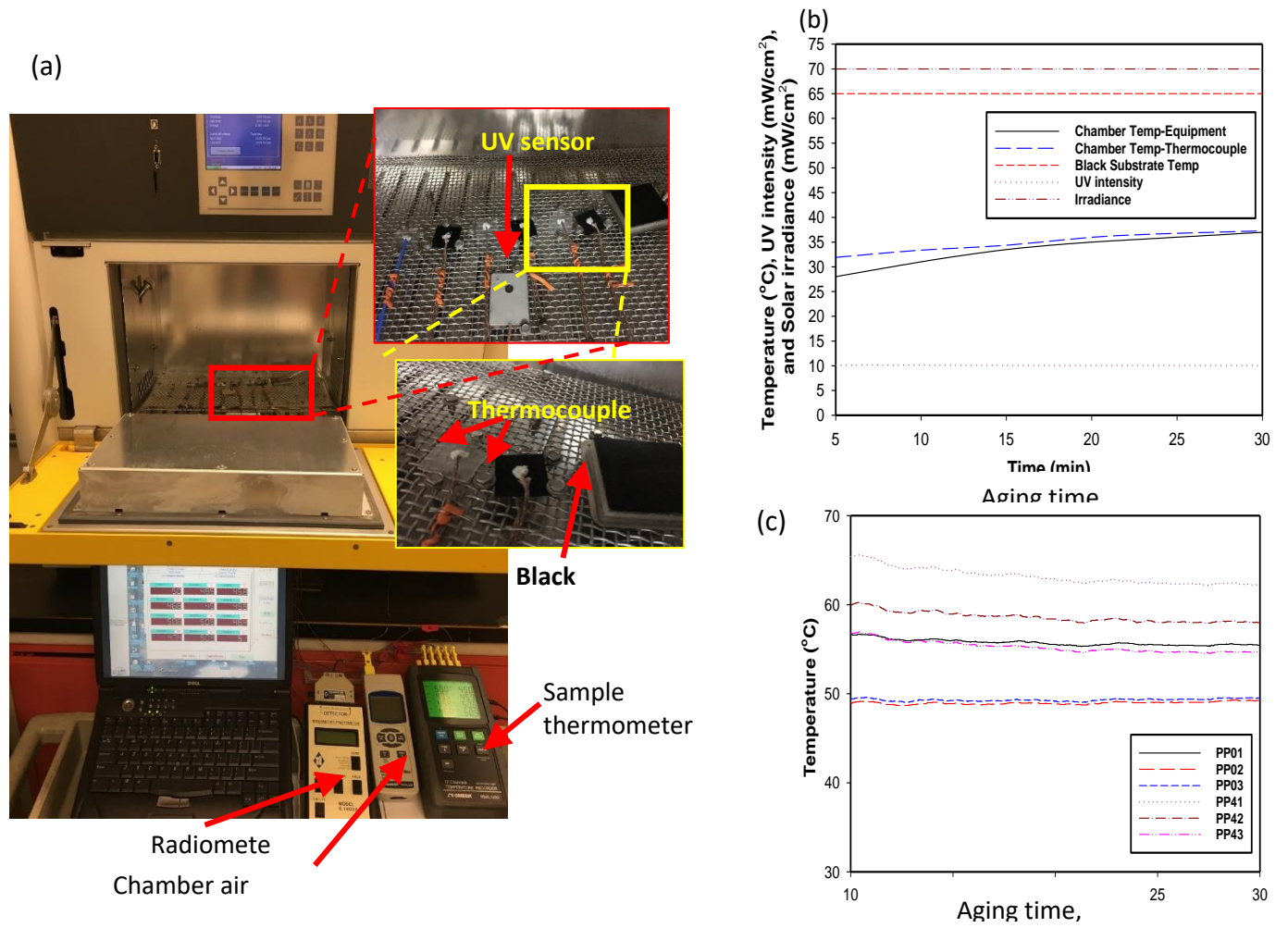


Figure S3 Accelerated weathering chamber and temperature profile of PP-CNT plate during Weathering (a) solar aging chamber, (b) Chamber Conditions during Weathering, (c) Sample Temperatures during Weathering

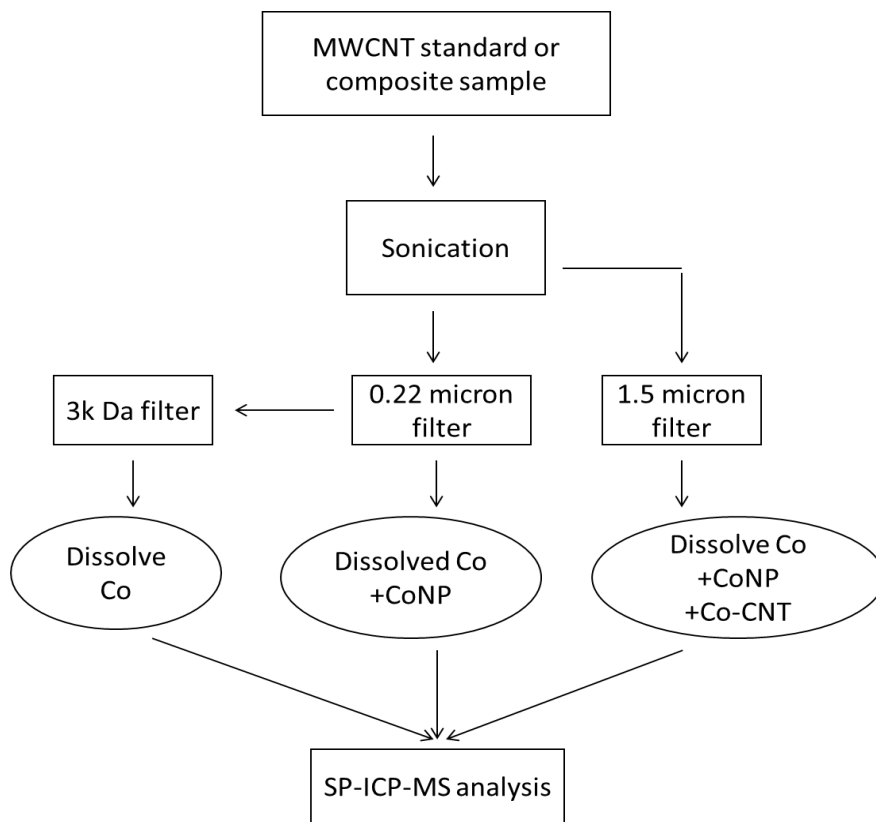


Figure S4 MWCNT standard and composite sample preparation and analysis procedure flow chart

S3. Analysis of MWCNT Released from Polymer Matrix using SP-ICP-MS

The use single particle (SP)-ICP-MS has shown to be a highly sensitive emerging technology for the analysis of metallic nanoparticle analysis in different matrices. Unfortunately, the common nanomaterials, carbon nanotubes (CNTs), filled to polymers to improve polymer's properties, cannot be detected by SP-ICP-MS directly. However, CNTs can be detected by monitoring metal nanoparticles that used as catalysts for their preparation. In this study, we developed SP-ICP-MS method to detect MWCNT leaching from polymers by tracking cobalt nanoparticle (CoNP) that used for producing MWCNT. The commercial multi-walled CNT (MWCNT 7000) has an average 1.5 μm length, Cobalt (NP ~ 10 nm, $\sim 60\%$ passed through 0.22 μm filter that were not attached to MWCNT, and Co ion. There was no Co detected that passed through 3000 Da molecule cutoff membrane.

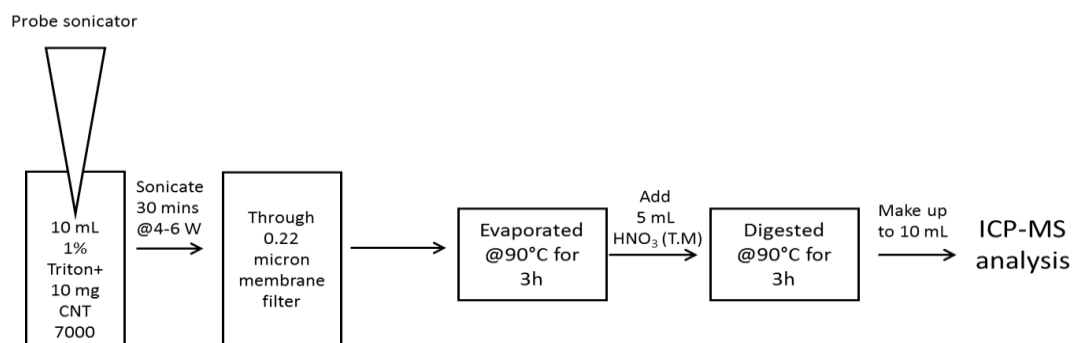


Figure S5 Flow chart for detection of Cobalt nanoparticle embedded/dissociated from MWCNTs

The instrument used was ICP-MS (PerkinElmer NexION 350 ICP-MS) with platinum cone, with SeaSpray nebulizer, and 1600 W plasma power. The gas flow in the Nebulizer was 1.00-1.02 L/min, transport efficiency 9.00 ± 1.00 % and sample flow rate 0.320 ± 0.020 mL/min and analyte used was cobalt (59). The dwell time in the analysis was 100 μs and scan time 100s.

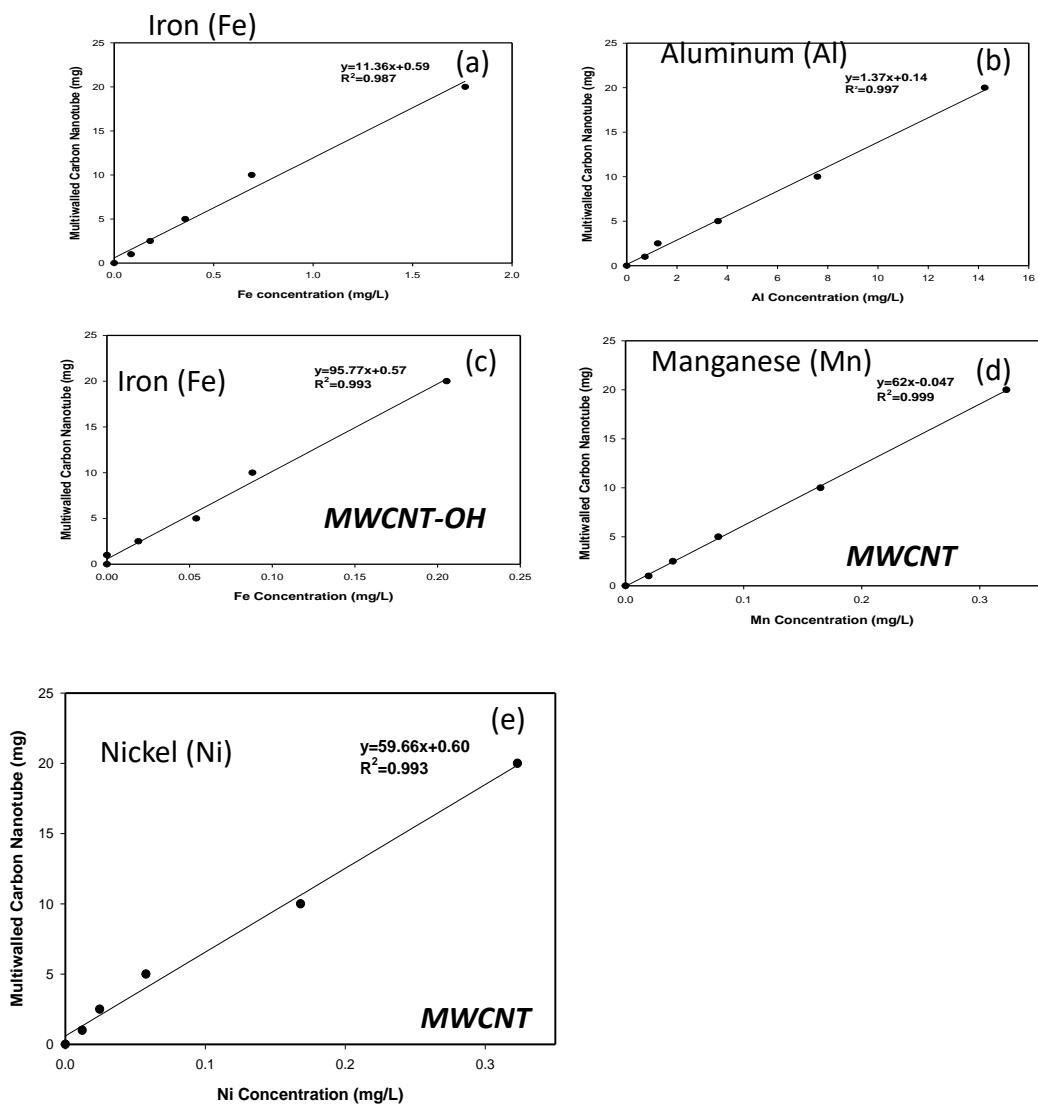


Figure S6 Calibration curve to quantify multiwalled carbon nanotube (MWCNT) (nanocyl 7000) using metal elements in MWCNT

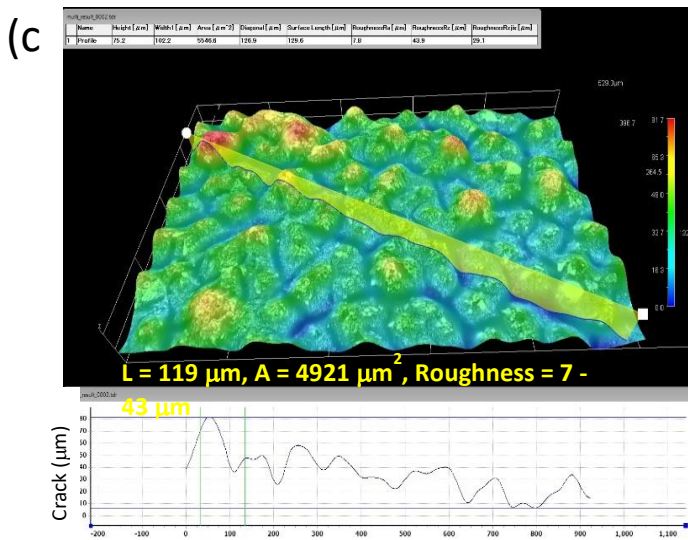
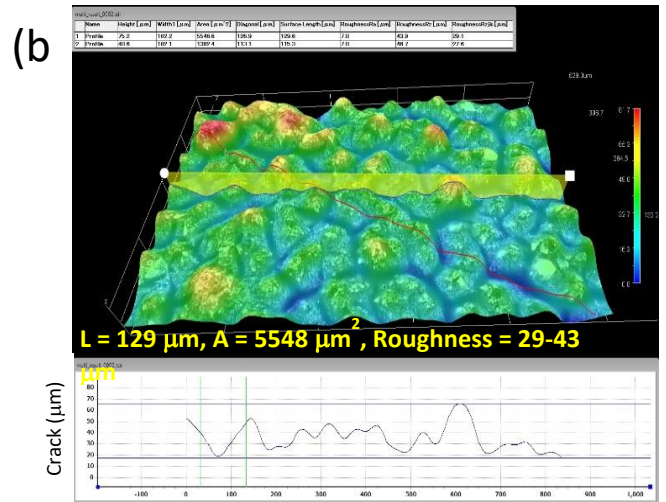
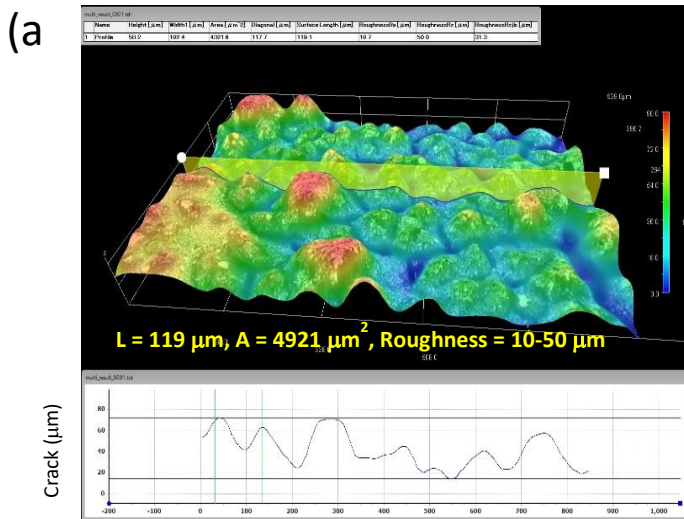


Figure S7 Digital optical image for surface characterization by Hirox 3D digital microscope which help visualize surface of aged polypropylene-MWCNT after 2268 h (a) PP41, (b) PP42, and (c) PP43

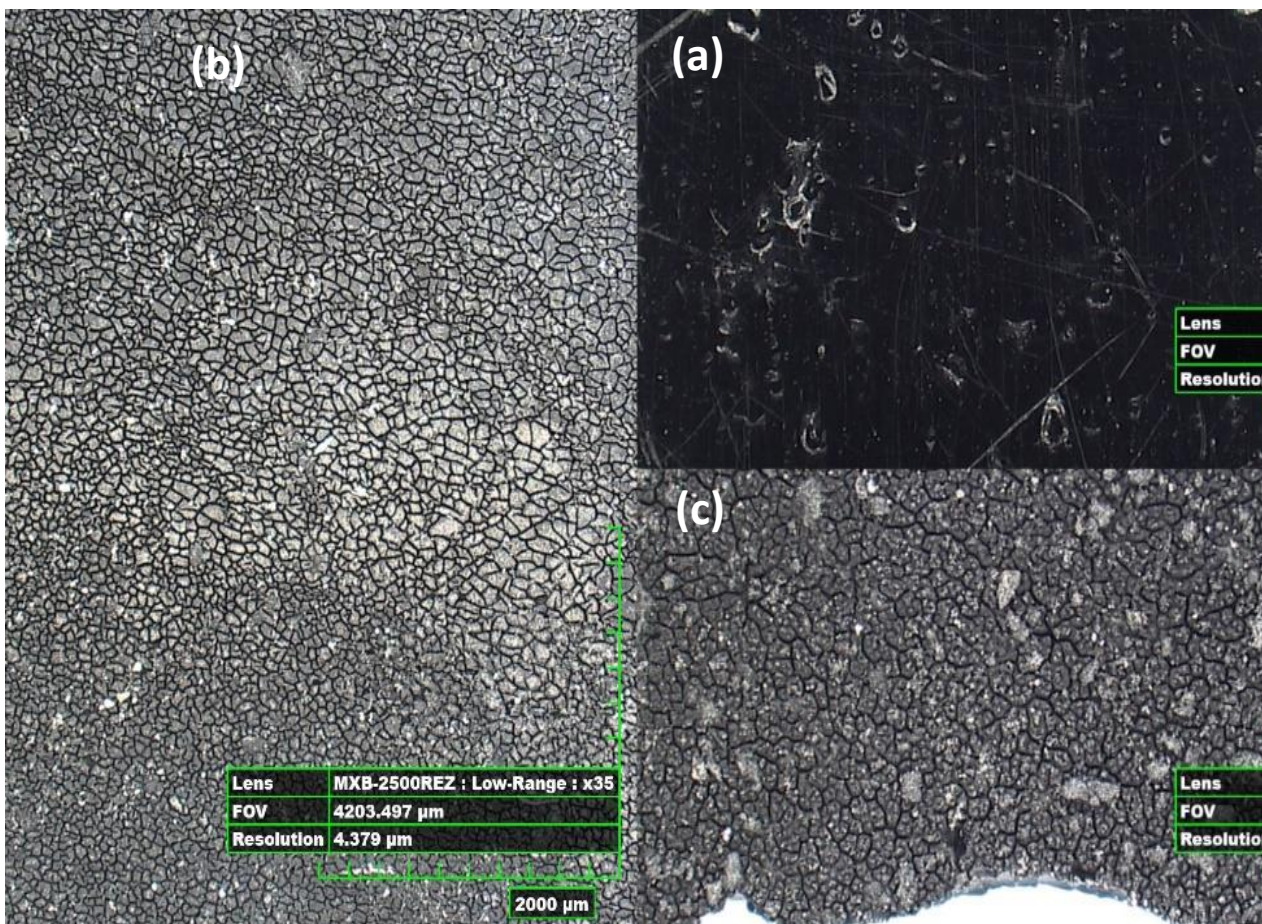


Figure S8 High resolution optical images (2000 X) of polypropylene-MWCNT showing local microstructural inhomogeneity (a) pristine PP41, (b) Environmental stress cracking after 2268 h showing craze formation and crack development, (c) after 3024 h

Table S1 Change in surface hardness of Polypropylene-CNT with environmental aging

	Aged Sampletime (h)	Hardness (a.u.)	Note	Sample	Aged time (h)	Hardness (a.u.)	Note
P43	0	43.3		P03	0	22.7	
	756	26.5			756	-14.3	
	1512	19.2			1512	N.A.	Sample brittle broken at contact
	2268	-3.6			2268	N.A.	Sample brittle broken at contact
P42	0	36		P02	0	-24.4	
	756	32.9			756	-245	Sample brittle broken at contact
	1512	-96.6	sample was slightly broken		1512	N.A.	Sample brittle broken at contact
	2268	-223	sample was broken during analysis		2268	N.A.	Sample brittle broken at contact
P41	0	41.5		P01	0	-34.8	
	756	28.6			756	N.A.	sample was broken at contact
	1512	-151	sample was broken during analysis		1512	N.A.	sample was broken at contact
	2268	N.A.	sample was broken at contact		2268	N.A.	sample was broken at contact

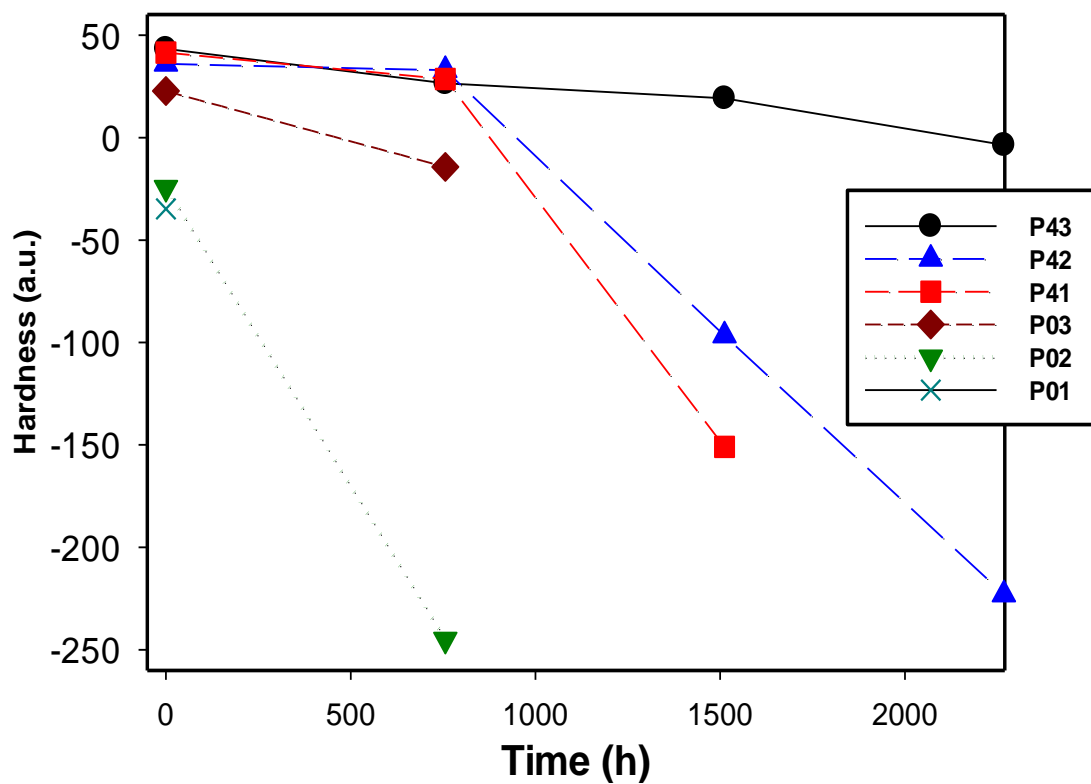


Figure S9 Change in hardness of Polypropylene-CNT as a function of environmental aging time

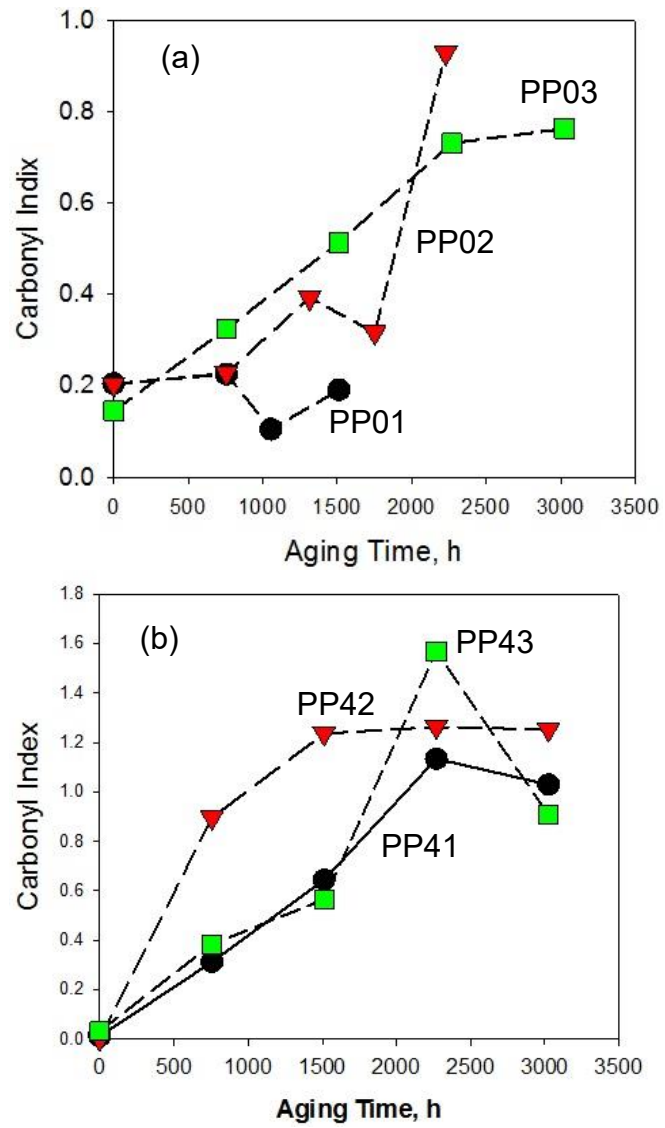


Figure S10 Carbonyl Index based on IR absorbance ratio of carbonyl groups (-OC-) at 1775 nm and methylene groups (-CH₂-) at 2879 nm for surface analysis (a) PP (b) PP-MWCNT

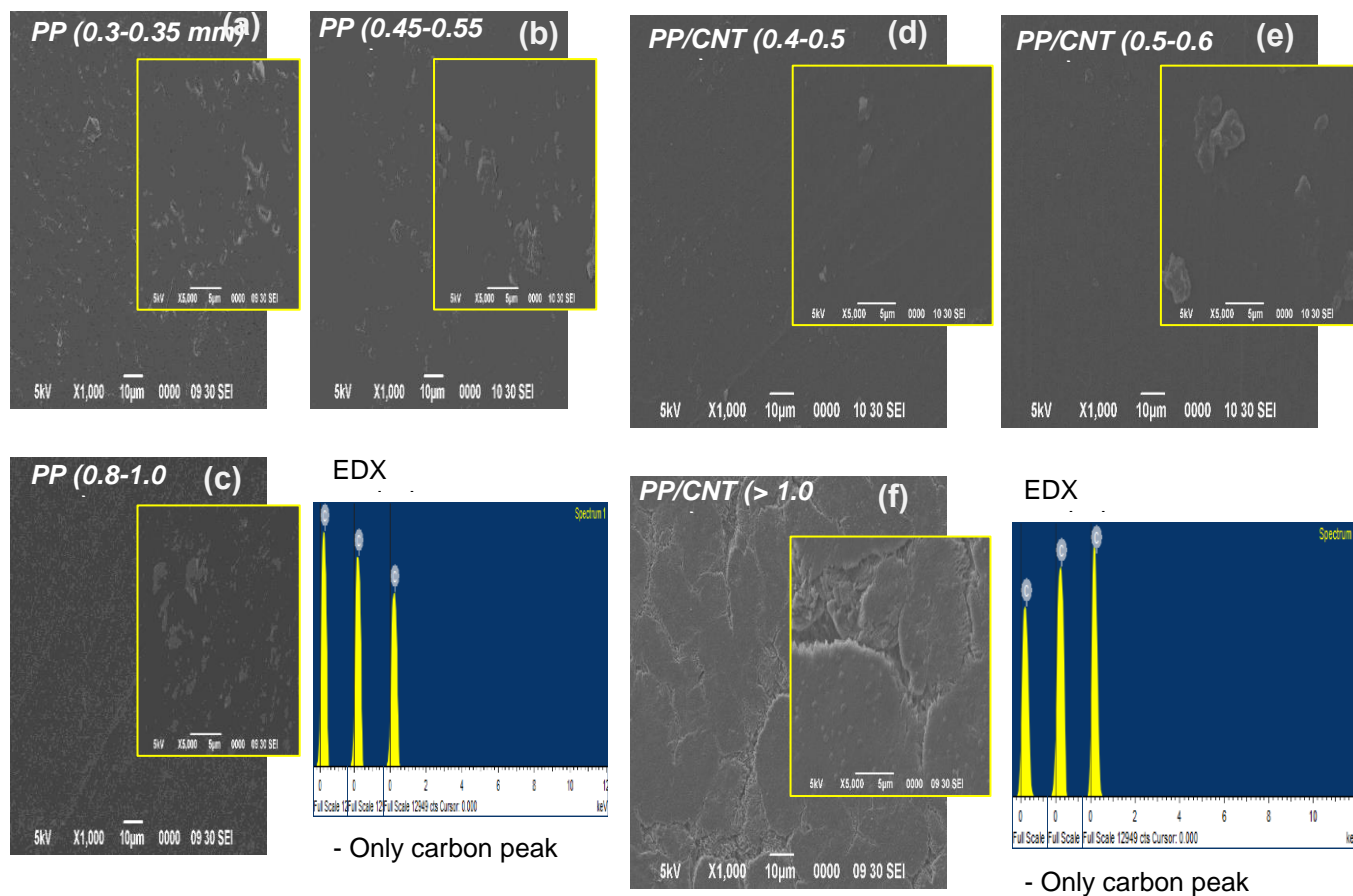


Figure S11 Scanning electron microscope images with energy dispersive X-ray spectroscopy showing surface topography and structure of polypropylene (a) PP01, (b) PP02, (c) PP03, and polypropylene-MWCNT composites (d) PP41, (e) PP42, and (f) PP43

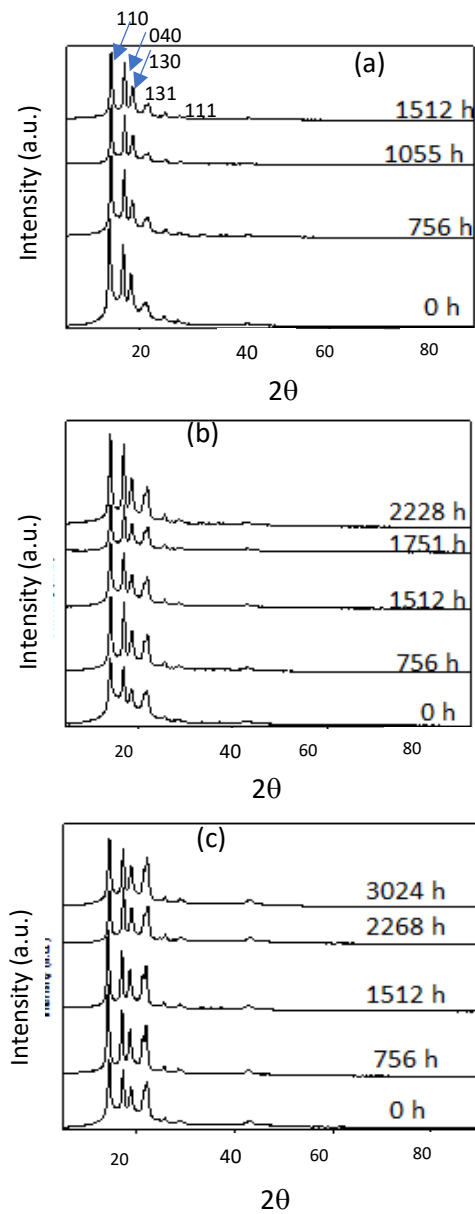


Figure S12 Structural analysis of polypropylene using X-ray powder diffraction technique as a function of the number of cycles and aging time for (a) PPO1, (b) PPO2, and (c) PP03

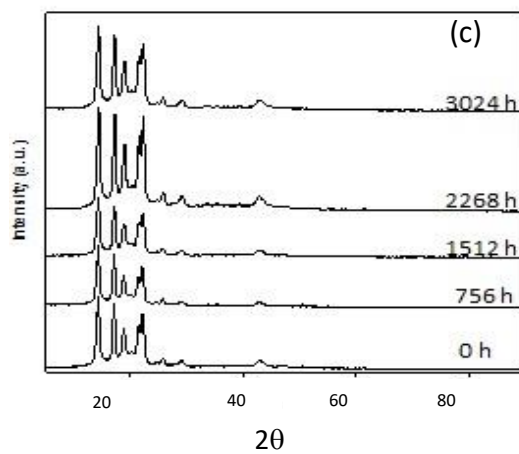
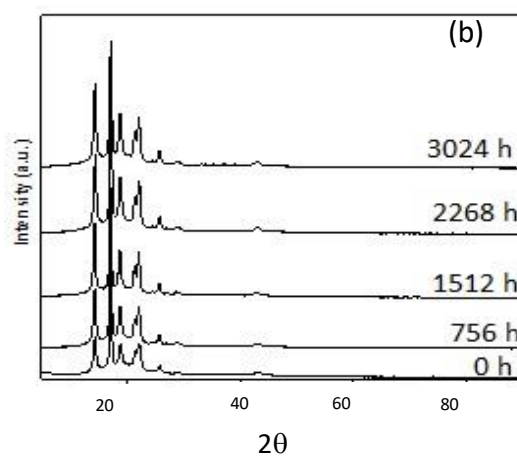
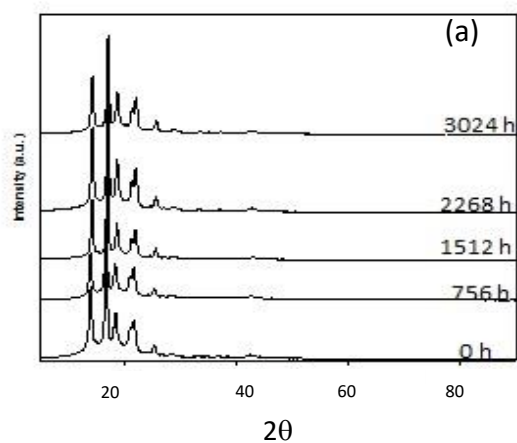


Figure S13 Structural analysis of polypropylene using X-ray powder diffraction technique as a function of the number of cycles and aging time for (a) PP41, (b) PP42, and (c) PP43

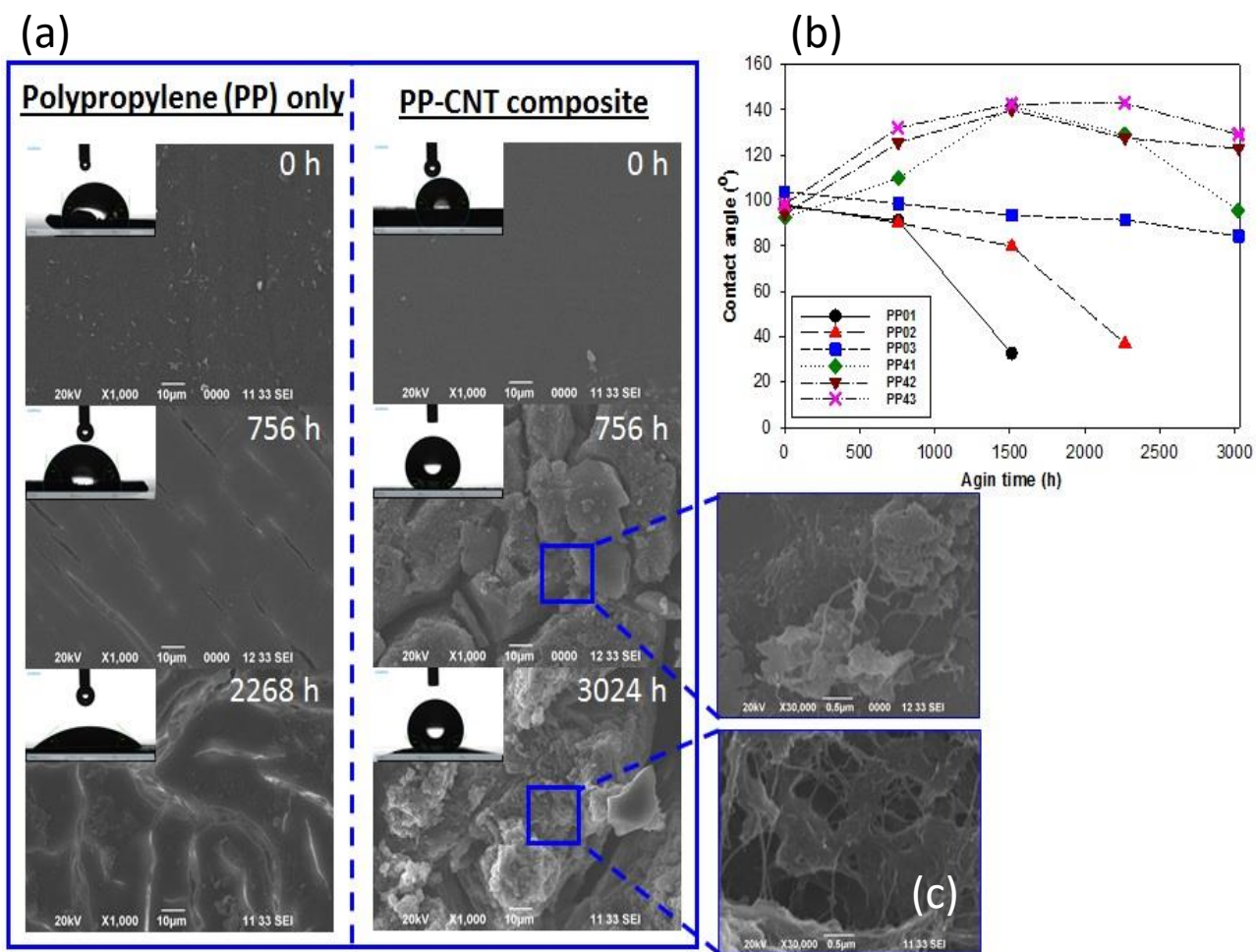


Figure S14 (a) Changes in contact angle changes during aging of PP and PP-MWCNT surfaces after selected degradation times, showing surface oxidation and erosion, (b) summary of contact angle for all samples as a function of aged times for all the samples

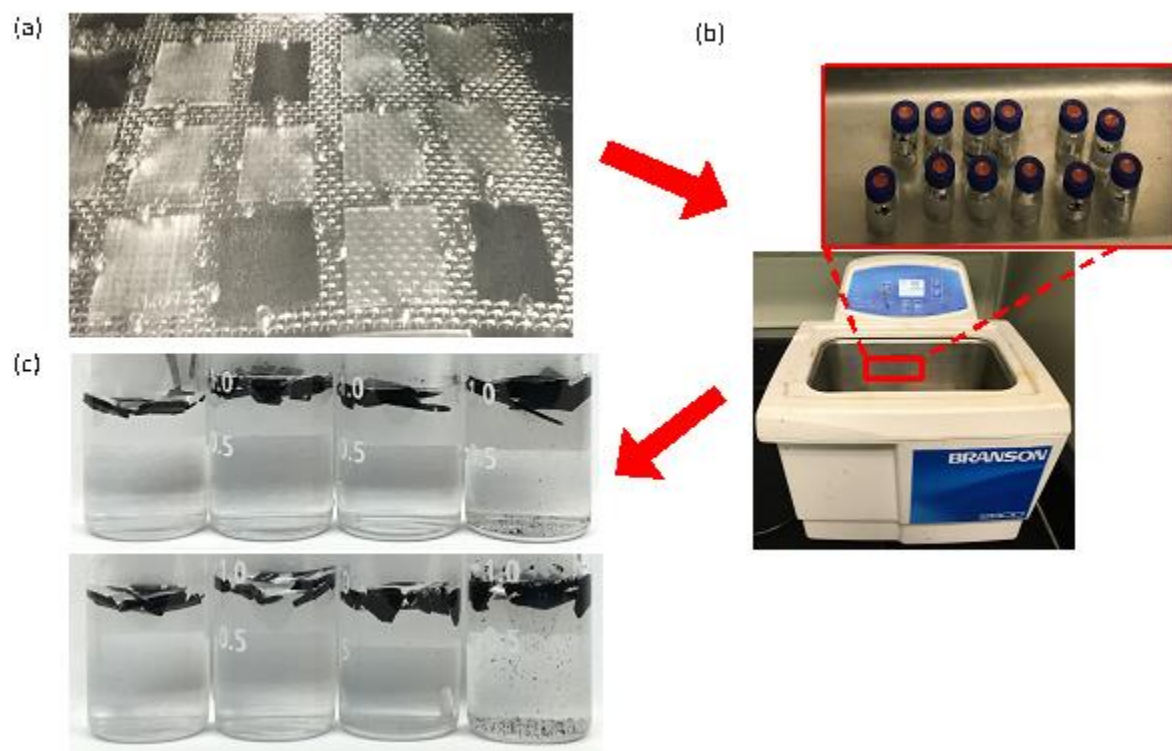


Figure S15 (a) Polypropylene (PP) and PP-carbon nanotube samples arranged for aging in the Atlas **SUNTEST** XXL⁺ weathering chamber.(b) sonication bath used for nanorelease studies, Each sample of 20 mg was added in 1.0 mL DI water and then sonicated for 30 min. (c) samples of aged polymer composites floating in wash water and released fragments of plastics and microplastics

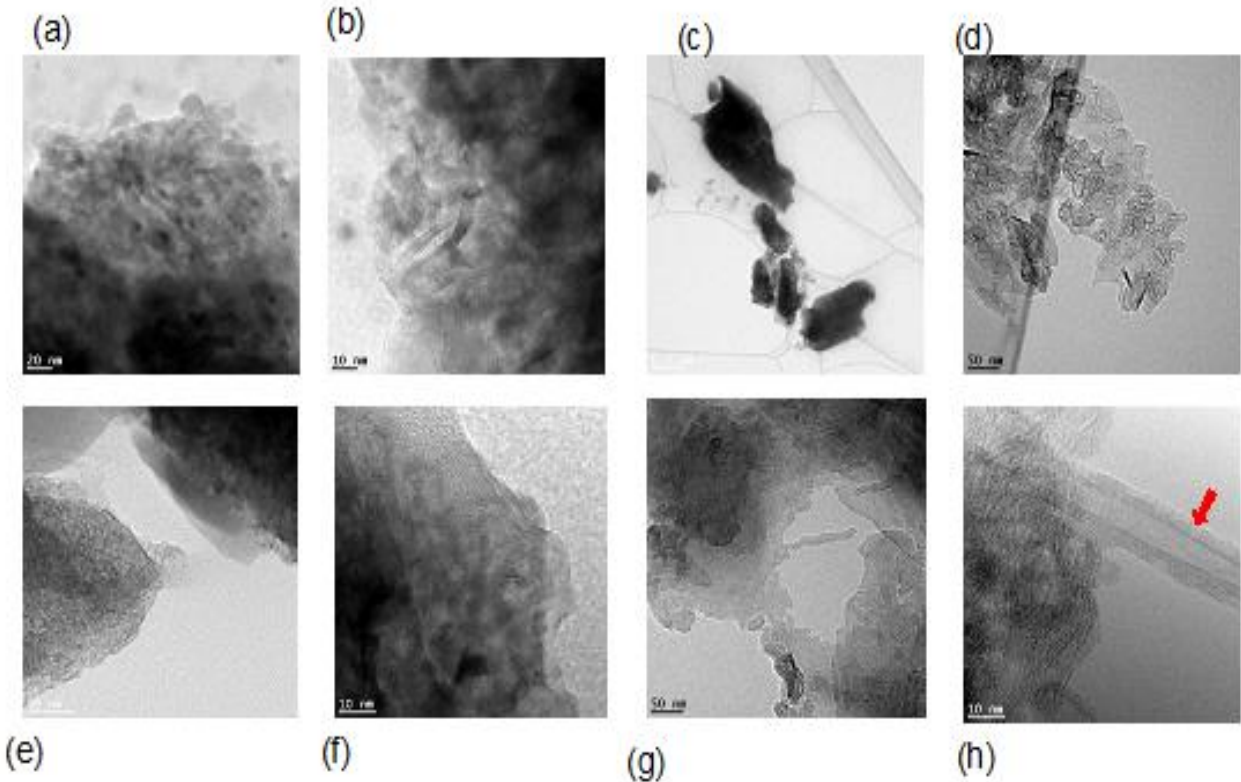


Figure S16 Transmission electron microscopy images of released polymer fragments and carbon nanotubes from aged PP-MWCNT composites